IJE TRANSACTIONS B: Applications Vol. 39, No. 02, (February 2026) 547-560

International Journal of Engineering

Journal Homepage: www.ije.ir

Finite Element Analysis of Multiaxial Fatigue and Mixed-Mode Crack Growth in Inconel 600

A. Moradi[a], K. R. Kashyzadeh*[b], M. Chizari[a]

[a] *School of Physics, Engineering & Computer Science, University of Hertfordshire, Hatfield AL10 9AB, UK*
[b] *Department of Transport Equipment and Technology, Academy of Engineering, RUDN University, 6 Miklukho-Maklaya Street, Moscow, Russian Federation*

PAPER INFO

Paper history:
Received 02 January 2025
Received in revised form 17 February 2025
Accepted 27 February 2025

Keywords:
Multiaxial Fatigue Life
Hysteresis Diagram
Mixed Mode Crack Growth
Inconel 600

ABSTRACT

This study investigates the fatigue life prediction of Inconel 600 under multiaxial loading conditions as well as fatigue crack growth under mixed mode (I and II). Finite element simulations based on critical plane criteria were performed for fatigue analysis under combined tensile and shear loading in different non-proportional modes (i.e., phase difference between tensile and shear loads). To achieve this, fully reversed tensile stress with a maximum value of 480 MPa (mean stress: zero) was considered. Subsequently, a constant shear stress of 28 MPa was applied at different phase angles ranging from 0° to 90° in 10-degree intervals (i.e., $0°\leq\theta\leq90°,\Delta\theta=10°$). For all modes, hysteresis stress diagrams were extracted to investigate the cyclic behavior of the material. Furthermore, various fatigue damage models, including Fatemi-Socie, SWT, normal strain, and shear strain, were employed to assess the fatigue life of the samples under different loading modes using MSC software. The results showed that the Fatemi-Socie and shear strain criteria predict the shortest fatigue life for phase difference in the ranges of 0°-30° and 40°-90°, respectively. Therefore, selecting a more conservative criterion is not feasible as it depends on the loading conditions. Additionally, it was found that the most critical conditions occurred at phase difference of 50° and 60°. Next, in order to numerically investigate the crack growth behavior, a semi-Arcan fixture model was used. Simulations were performed for four different loading modes (i.e., fixture settings), considering variations in the loading angle with respect to the longitudinal axis of the crack (0°, 30°, 60°, and 90°). Eventually, crack length graphs were extracted in terms of loading cycles. The results indicated that the lowest and highest crack growth rates occurred when the angle between loading and the longitudinal axis of the crack was 0° and 90°, respectively.

***doi**: 10.5829/ije.2026.39.02b.20*

Graphical Abstract

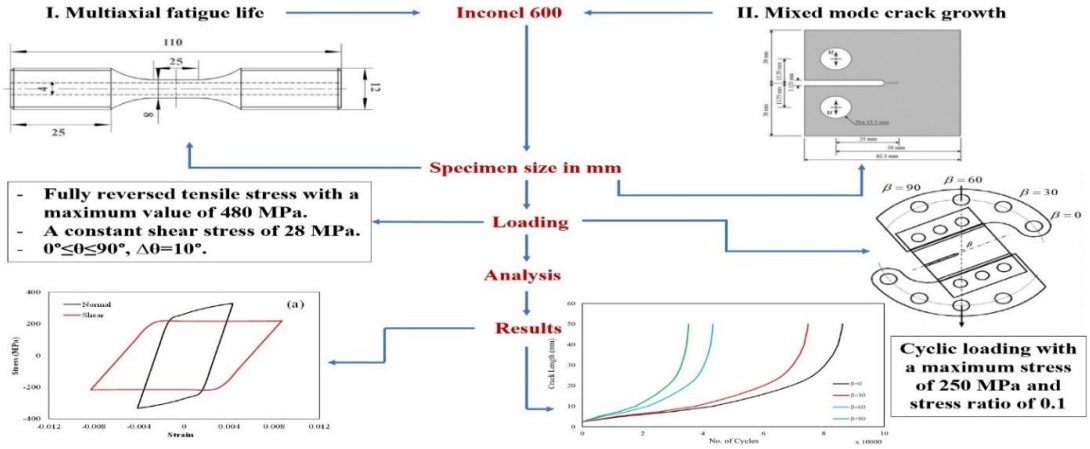

*Corresponding Author Email: reza-kashi-zade-ka@rudn.ru (K. Reza Kashyzadeh)

Please cite this article as: Moradi A, Kashyzadeh KR, Chizari M. Finite Element Analysis of Multiaxial Fatigue and Mixed-Mode Crack Growth in Inconel 600. International Journal of Engineering, Transactions B: Applications. 2026;39(02):547-60.

ABBREVIATIONS			
Ni	Nickel	SWT	Smith-Watson-Topper
Cr	Chromium	MSS	Maximum Shear Stress
Fe	Iron	FSS	Fatigue Shear Stress
HCF	High-Cycle Fatigue	NSS	Normalized Shear Stress
LCF	Low-Cycle Fatigue	SIF	Stress Intensity Factor
FCG	Fatigue Crack Growth	FEM	Finite Element Model

1. INTRODUCTION

Inconel materials are Nickel (Ni)-Chromium (Cr)-Iron (Fe) alloys, often referred to as high temperature steels. In fact, they are an effective choice for high-temperature operation in power plant components (1), with significant resistance to chemical degradation, high strength at high temperatures, resistance to wear and corrosion, good weldability (2), and other excellent mechanical properties. Despite these advantages, Inconel materials are not immune to damage. On the other hand, in various industries, material failure under cyclic loads remains a fundamental challenge. According to researchers, fatigue is the primary cause of failure in mechanical components (3, 4), necessitating durability and safety evaluations under different working conditions (5-8).

Industrial studies indicate that components experience complex loadings, and their strength assessment under simplified conditions may lead to unrealistic results (9). Hence, fatigue analysis must be performed under realistic conditions, i.e., in a multiaxial manner (10). In other words, multiaxial fatigue involves cyclic stresses in multiple directions, making it significantly more complex than uniaxial fatigue, which applies stress in a single direction. Several key parameters influence multiaxial fatigue analysis, including:

- Stress amplitude and mean stress (11);
- Loading path (12);
- Environmental factors (e.g., temperature);
- Microstructural characteristics (13).

Although there are more influential parameters, the most important ones were mentioned above.

Experimental results show that higher stress amplitudes generally reduce fatigue life. Moreover, mean tensile stresses shorten fatigue life more than mean compressive stresses (14, 15). Additionally, the path of applied load, whether proportional or non-proportional, significantly affects fatigue life. In this regard, non-proportional loading paths, where stress direction and magnitude change during cycles, tend to cause more damage (16-18). High temperatures, commonly encountered in Inconel applications, accelerate fatigue damage through oxidation and other degradation mechanisms (19, 20). Furthermore, it has been found that the microstructure of Inconel materials, including grain size and phase distribution, plays a crucial role in fatigue behavior. Fine-grained microstructures enhance fatigue resistance by increasing barriers to crack propagation (21-23). Numerous studies have been conducted on Inconel fatigue life estimation under different conditions and considering different effective factors. Moreover, experimental studies involving the influence of various parameters on the fatigue crack growth rate in Inconel materials are abundant (24-28).

However, analyzing all possible scenarios, including mutual effects of multiple parameters, remains a challenge due to cost and time constraints in industrial projects. Inconel raw material is expensive, and its manufacturing process incurs higher costs than other steels. Additionally, replicating real working conditions in laboratory settings is difficult and sometimes impossible. Even if performed successfully, multiaxial fatigue tests alone are costly and time-consuming. Due to these limitations, in recent decades, researchers have increasingly relied on numerical simulations using finite element software. These tools offer powerful capabilities for fatigue analysis, providing an efficient alternative to costly experiments. However, accurate and reliable results from finite element simulations require specialized expertise. Additionally, finite element models must be validated, usually by comparing simulation results with published scientific data or real experimental results. An example of the use of software in solving complex fatigue problems, Rasul et al. (29) explored the multi-objective optimization of stress concentration factors for fatigue design in internal ring-reinforced KT-joints undergoing brace axial compression. Their findings highlight the importance of stress distribution in fatigue life estimation. Similarly, Major et al. (30) analyzed the heating effects on steel structures under fire load, which provides insights into material behavior under extreme conditions, relevant for understanding fatigue performance in high-temperature environments. Recent research has also explored fatigue crack growth in structures subjected to coupled fluid-structural vibrations (31). These studies contribute valuable perspectives to the existing body of knowledge on fatigue analysis.

From the above literature review, a major challenge in evaluating fatigue life and crack growth in Inconel 600 is the complexity of multiaxial stress states, where interactions between tensile and shear stresses create non-proportional loading conditions. Traditional fatigue

analysis methods, which rely heavily on uniaxial testing, fail to capture these complexities, leading to inaccurate life predictions. Furthermore, experimental fatigue testing is expensive, time-consuming, and often impractical for investigating multiple loading scenarios and material behaviors. To overcome these limitations, numerical simulations using finite element analysis (FEA) have gained prominence as a viable alternative. The present study focuses on developing and validating a finite element model to predict multiaxial fatigue life and mixed-mode crack growth behavior in Inconel 600. The key contributions of this work include:

1. Implementing advanced fatigue damage models, including Fatemi-Socie and SWT criteria, to accurately assess fatigue life under complex loading conditions.
2. Investigating non-proportional loading effects by varying phase angles between tensile and shear stresses.
3. Analyzing mixed-mode crack propagation using a semi-Arcan fixture to study crack growth in different loading orientations.
4. Providing a validated, cost-effective numerical framework for predicting fatigue behavior, reducing reliance on costly experimental tests.

The structure of this study is as follows: Section 2 describes the theoretical basis of different criteria used in the current research. Section 3 presents the details of finite element models, including multiaxial fatigue and crack growth in mixed mode. Section 4 analyzes the Finite Element (FE) results. Finally, section 5 presents the conclusions of the study.

2. THEORETICAL BASIS OF DIFFERENT CRITERIA USED IN CURRENT RESEARCH

2. 1. Critical Plane Approaches Critical plane approaches are widely used to predict the fatigue life of components under multiaxial (proportional or non-proportional) loading conditions. When a material undergoes cyclic loading in multiple directions, it experiences complex stress states that significantly impact its fatigue life. In such cases, conventional methods based solely on stress or strain amplitude often fail to provide a accurate fatigue life predictions, sometimes resulting in errors of up to 100%. Additionally, complex geometries can further complicate the stress distribution, leading to non-proportional stress relationships even when simple axial loads are applied. Critical plane approaches address these challenges by identifying the material plane where the highest destructive stresses occur during the loading cycle.

This critical plane represents the location most susceptible to fatigue damage, initiating and propagating cracks (32, 33). The concept behind critical plane approaches is that fatigue failure is primarily driven by the stress state on this critical plane rather than the individual stress components. Various mathematical criteria, such as Maximum Shear Stress (MSS), Fatigue Shear Stress (FSS), and Normalized Shear Stress (NSS), are used to determine this plane. These criteria assess the amplitude and phase relationship of principal stresses across multiple plans to identify the most critical one. Once the critical plane is established, fatigue life is estimated using damage accumulation models, such as the Rainflow counting method combined with Miner's rule. These models track the cumulative damage caused by each stress cycle on the critical plane to predict the total fatigue life of the component. However, it is important to explore other feasible alternatives and justify the choice of the critical plane approach in this study. In this regard, the following approaches can be mentioned:

- Stress Invariant-Based Methods: These methods, such as the von Mises equivalent stress approach, rely on stress invariants to estimate fatigue life. They are computationally efficient but do not account for the directional dependence of multiaxial stresses, leading to potential inaccuracies in complex loading conditions.
- Energy-Based Methods: Approaches like the Wang-Brown energy-based model evaluate fatigue life by considering the total strain energy absorbed during cyclic loading. While effective in capturing both stress and strain effects, they require extensive material testing to calibrate model parameters accurately (4).
- Empirical and Machine Learning Models: Recent advancements include data-driven models trained on experimental data to predict fatigue life (34). These methods can be highly adaptable but require large datasets and may lack interpretability in physical terms.

Therefore, one of the most important reasons for using the critical plane approach over the above methods for this study is to consider the effects of non-proportional loading.

2. 1. 1. Fatemi-Socie Model The Fatemi-Socie model, developed in the late 1980s, is widely used to predict fatigue life under multiaxial loading (35). It refines earlier fatigue models by incorporating the concept of the critical plane, which is the plane where fatigue damage accumulates most rapidly. Unlike models that evaluate stress amplitude on a single plane, this approach considers the plan's orientation relative to principal stress directions. The Fatemi-Socie model integrates elements of both stress-based and strain-based fatigue criteria. It evaluates fatigue damage based on equivalent strain amplitude, taking into account mean stress, stress amplitude, and the interaction between shear

and normal stresses on the critical plane. The critical plane is identified by aligning the principal stress direction with the coordinate system axes, followed by calculating the strain components and the equivalent strain range is determined by the combination of these components. This model utilizes experimental fatigue coefficients and equations to estimate fatigue life based on the equivalent strain range. The Fatemi-Socie model is expressed by the following equation (35):

$$\gamma_a(1+\left(\frac{\sigma_n}{\sigma_{ys}}\right)) = (\tau_f{}'/\mathrm{G})(2N_{fs})^b + \gamma_f{}'(2N_{fs})^c \quad (1)$$

in which, $\tau_f{}'$ represents the coefficient of shear fatigue strength, G is the shear modulus of the material, $\gamma_f{}'$ is the torsional fatigue strength coefficient, and b and c are material constants. Additionally, σ_n is the normal stress on the critical plane, σ_{ys} is the yield stress of the material, and γ_a is the shear strain amplitude.

2. 1. 2. SWT Model Based on Critical Plane Approach The Smith-Watson-Topper (SWT) model assumes that fatigue failure is governed by the nucleation and growth of fatigue cracks on the critical plane. It estimates fatigue life under multiaxial loading conditions, considering a combination of tension, compression, torsion, and shear. According to this model, failure occurs on the plane where the parameter $d_t = \varepsilon_a\sigma_n$ has its maximum value, and this plane is referred to as the critical plane.

The equation used based on this model is as follows:

$$d_t = ((\sigma_f{}')^2/E)(2N_{ft})^{2b} + \varepsilon_f{}'\sigma_f{}'(2N_{ft})^{b+c} \quad (2)$$

The SWT model is specifically designed to predict the fatigue life of metallic materials under complex multiaxial loading conditions. It accounts for the interaction between normal and shear stresses on the critical plane, similar to the Fatemi-Socie model. This model considers both High-Cycle Fatigue (HCF) and Low-Cycle Fatigue (LCF) regimes while also incorporating the effects of mean stress. In the equation above, ε_a and σ_n represent the normal strain and normal stress amplitude on the critical plane, respectively.

2. 2. Fatigue Crack Growth (FCG) Fatigue crack growth occurs in materials subjected to cyclic loading, leading to the gradual propagation of cracks. This phenomenon is a major failure mode in structural components, making it a critical factor in engineering design and maintenance. Under cyclic loading, cracks typically initiate at high-stress regions, such as notches or pre-exiting flaws. These microcracks grow incrementally with each loading cycle. Fatigue crack growth depends on factors such as cyclic loading magnitude, Stress Intensity Factor (SIF) at the crack tip, and the material fracture toughness. FCG behavior is commonly characterized by a relationship between the crack growth rate (da⁄dN) and the range of crack-tip stress intensity factor (ΔK). The stress intensity factor K depends on the crack length a, loading type, and geometry. A typical relationship between da⁄dN and ΔK in a log-log plot can be illustrated in Figure 1 (36), and it can be expressed by the Paris equation as follows (37):

$$\frac{da}{dN} = C(\Delta K)^m \quad (3)$$

where da⁄dN is the crack growth rate, ΔK is the stress intensity factor range, and C and m are material-specific constants determined through experimental calibration. For ductile materials, m typically ranges from 2.5 to 5.5 (38-42), whereas for brittle materials, it varies between 8 and 10 (43).

A significant factor influencing fatigue crack growth and also the overall fatigue life of components is the loading ratio (i.e., minimum to maximum load ratio) (44, 45). The fatigue crack growth rate is generally higher in tension than in compression, a phenomenon known as the R-ratio effect. In real, tensile stresses accelerate crack propagation due to larger plastic zones at the crack tip, whereas compressive stresses inhibit growth by closing the crack slightly during loading cycles. Furthermore, at low R-values, fatigue crack growth is more pronounced due to the dominance of tensile stresses, whereas at higher R-values, growth rates decrease.

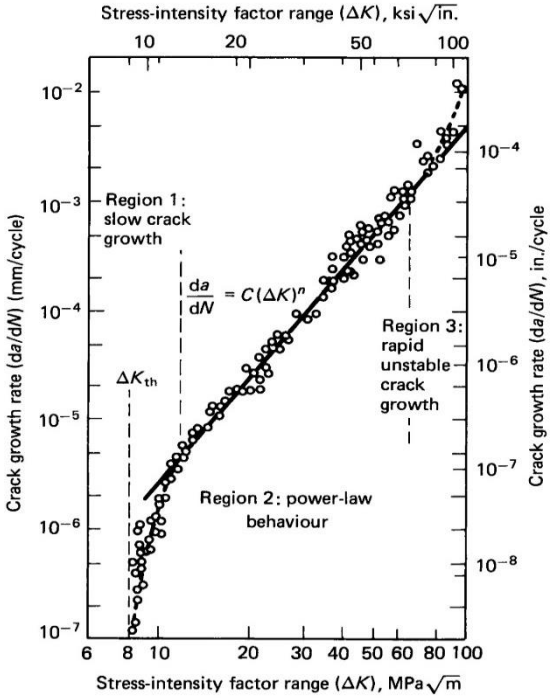

Figure 1. A typical representation of fatigue crack growth rate versus stress intensity factor range for a ductile material. Copyright with official permission from Elsevier [36].

3. SIMULATION PROCEDURE

To achieve the research objectives, three software programs, SOLIDWORKS, ABAQUS, and MSC FATIGUE, were utilized. First, 3D geometric models, including the standard fatigue test sample, the crack growth test sample, and the semi-Arcan fixture, were created in SOLIDWORKS. These models were then imported into ABAQUS, where material properties assigned, boundary and loading conditions were defined, and initial stress analysis was performed. Finally, the results from ABAQUS, along with the Finite Element Model (FEM), were imported into MSC software. After defining the fatigue properties of the material and cyclic loading conditions, calculations were conducted, and fatigue life was estimated using various criteria. It is worth noting that ABAQUS software was directly used to generate hysteresis diagrams and analyze crack growth.

3. 1. Geometry A thin-walled tubular specimen, modeled according to the ASTM E2207-08 standard (46), was used for the fatigue test. Figure 2 illustrates the geometry and dimensions of this multi-axial fatigue test sample (all dimensions are in mm). Moreover, a Compact-Tension (CT) sample was modeled for the FCG test, as shown in Figure 3 (47). Finally, the semi-Arcan fixture was modeled based on reference specifications (48, 49). Figure 4 displays the assembly of the CT sample in the fixture along with the different studied configurations.

3. 2. Material The material used in this research was Inconel 600 alloy. Its chemical composition is summarized in Table 1, while its physical and mechanical properties, as defined in the software, are listed in Table 2. The stress-strain diagram for this material is shown in Figure 5, where a bilinear plasticity model was employed to define the plasticity zone.

Then, to perform the fatigue analysis, the fatigue properties obtained from the axial test with zero stress ratio were applied (Figure 6). Also, the results obtained in the previous article were used to define the fatigue parameters (51).

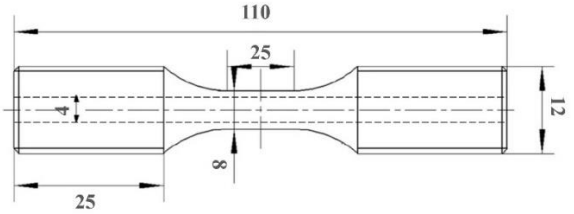

Figure 2. The size and geometry of the multi-axial fatigue test sample according to the ASTM E2207-08 standard (all dimensions are in mm)

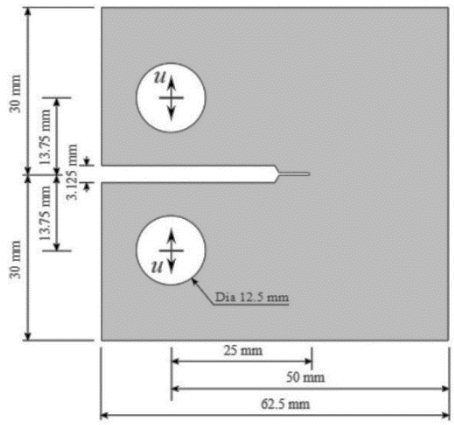

Figure 3. The size and geometry of the CT sample (all dimensions are in mm). Copyright with official permission from Elsevier (47)

TABLE 1. Chemical composition (%) of Inconel 600 (50)

Ni	Cr	Fe	C	Mn	S	Si	Cu
73.63	15.68	8.79	0.054	0.33	0.006	0.24	0.028

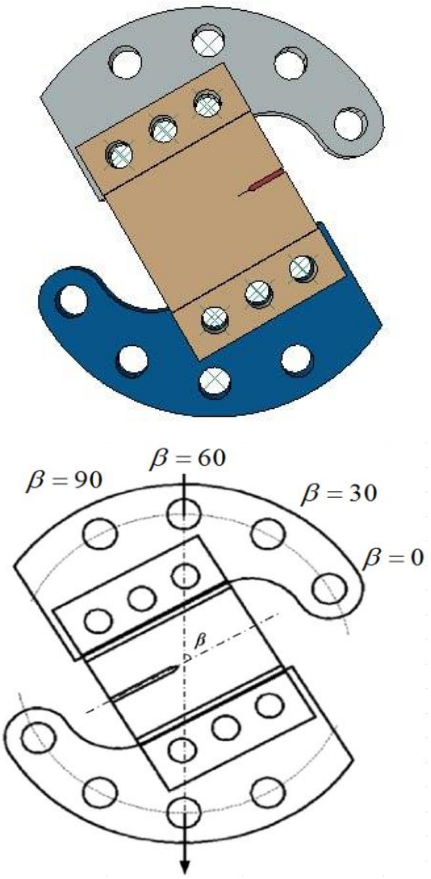

Figure 4. A view of the CT sample installation to the semi-Arcan fixture (top image) and different studied modes (bottom image)

TABLE 2. Mechanical properties of Inconel 600

Properties	Unit	Value
Elastic modulus	GPa	214
Shear modulus	GPa	80.8
Poisson's ratio	---	0.324
Density	Kg/m3	8470
Ultimate Tensile Strength (UTS)	MPa	671
Yield Strength (YS)	MPa	345
Elongation	%	50.8

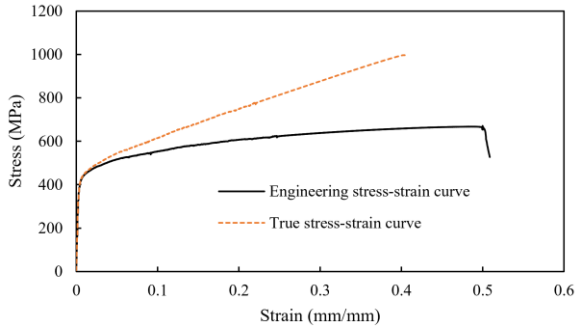

Figure 5. Engineering and true stress-strain curves for Inconel 600

3. 3. Mesh Process Meshing plays a crucial role in finite element modeling as influences the accuracy of the results (52). A manual meshing approach was adopted to ensure uniformity using square elements wherever possible. However, triangular elements were necessary for curved and cornered areas, such as fixture curves and crack tips.

Element C3D8R (8-node linear brick, reduced integration) was used to mesh standard fatigue specimens, while for extracting hysteresis diagrams, the selected elements must be able to handle large deformations, material nonlinearity, and provide accurate stress-strain behavior. Therefore, the previous element was considered as a 3D solid element. Also, due to the good compatibility of this element between the two softwares, i.e., ABAQUS and MSC FATIGUE, the same element was also used for meshing the standard CT sample. However, R3D4 (4-node 3D rigid element) was used to mesh the fixture. Furthermore, mesh convergence studies were conducted to verify that results were independent of the element count and size while maintaining manageable computational time. The target of stress changes with less than 1% variation was considered to determine the optimal element size. However, this constraint was not possible for the third analysis and after much effort, these variations were considered equal to 3% and less. Figure 7 shows the mesh convergence graphs for all three analyses.

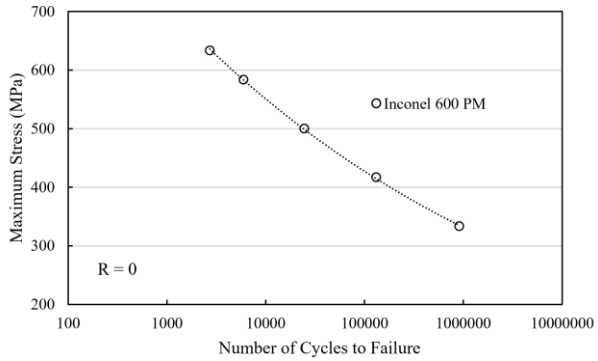

Figure 6. Fatigue test data for Inconel 600. Coptright Open Access under a Creative Commons (CC BY) license (51)

3. 4. Boundary Conditions Three different analyses were performed, each requiring specific boundary conditions:

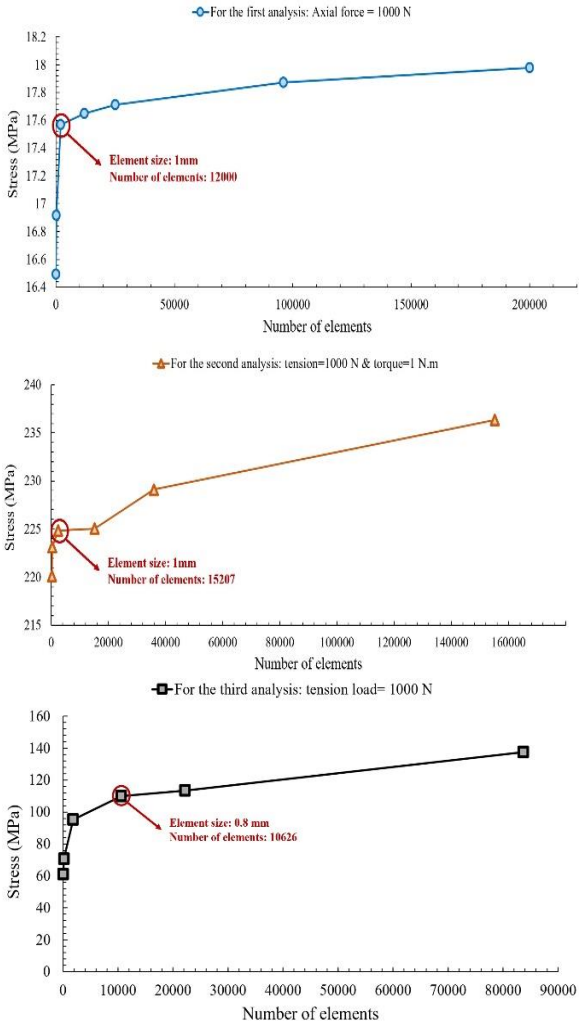

Figure 7. Mesh convergence graphs for all three analyses

1. Fatigue analysis to analyze the fatigue on the standard sample and extract the stress-life graph data, the bottom cross-section of the sample was fully constrained (fixed in all three translational and three rotational directions). The nodes in the upper cross-section were connected to a central node as a reference. After that, tensile axial force was applied to this reference node along the sample's length. Middle surfaces were only allowed to move longitudinally, restricting movement in five directions.
2. Multiaxial fatigue life evaluation: A fully reversed tensile stress with a maximum value of 480 MPa (mean stress: zero) was applied to the reference node. Then, a constant shear stress of 28 MPa was imposed at phase angles ranging from 0° to 90° in 10° increments.
3. Crack growth behavior analysis: Four loading modes were considered based on fixture settings, with variations in the angle between the applied load and the crack's longitudinal axis (0°, 30°, 60°, and 90°). A cyclic load with a maximum stress of 250 MPa and a stress ratio of 0.1 was applied, as shown in Figure 4.

3. 5. Analysis Stress analysis was perfomed using ABAQUS, and the resulting contours were extracted. MSC.FATIGUE software was then used to calculate fatigue life. The obtained results included the stress-life diagrams for the first analysis, hysteresis diagrams for the second analysis, and the crack length vs. loading cycles for the third analysis. These results are discussed in detail in the following section.

4. RESULTS AND DISCUSSION

4. 1. Validation To obtain S-N curve of the Inconel 600 standard specimen, the stress and strain distributions in the sample were obtained at each load level. The required stress and strain values obtained in a complete loading-unloading cycle were then utilized to predict fatigue lives according to the strain-based Basquin fatigue damage model (Equation 4) in the MSC.FATIGUE software. Finally, the predicted results were plotted versus the applied stresses to obtain the S-N curves.

$$\varepsilon_a = \sigma_f'(2N_f)^b + \varepsilon_f'(2N_f)^c \quad (4)$$

The values of the fatigue parameters in the above equation were substituted according to Section 3.2. The stress distributions along the longitudinal and transverse paths, and in the directions of S11 and S22 undergoing stress equals to 630 MPa are shown in Figure 8. Moreover, the von Mises stress, maximum principal strain, and S11 and S22 stress contours are also illustrated in Figure 9. Finally, a comparison between the stress-life

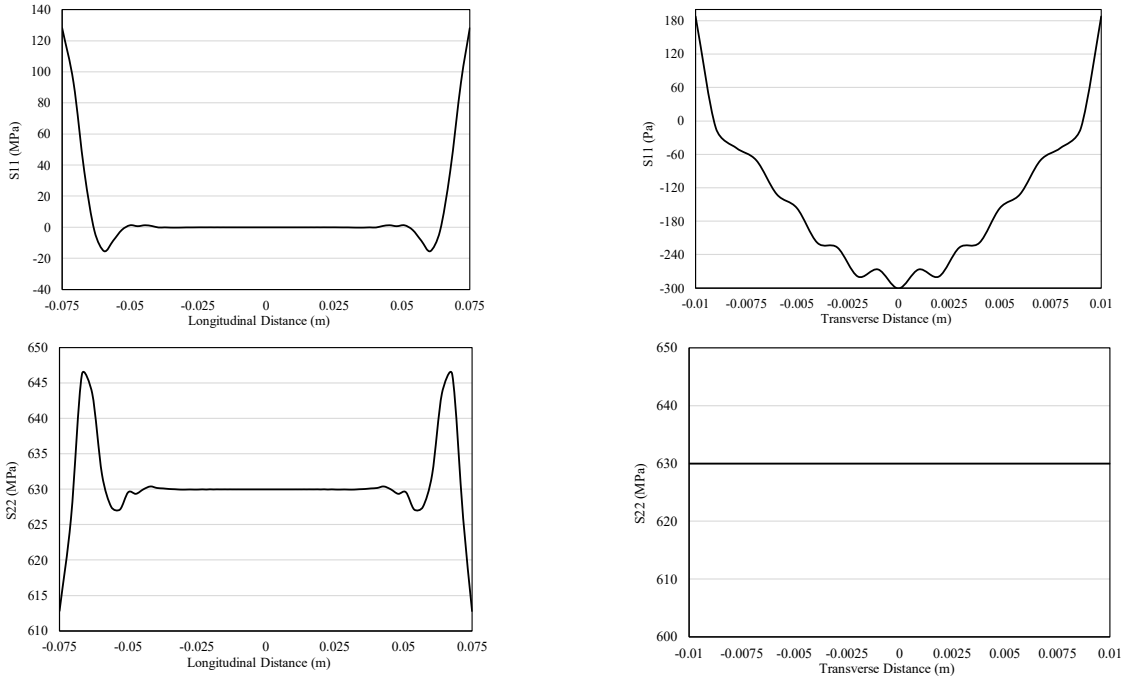

Figure 8. S11 and S22 stress distributions along the longitudinal distance (top left and bottom left), S11 and S22 stress distributions along the transverse path (top right and bottom right)

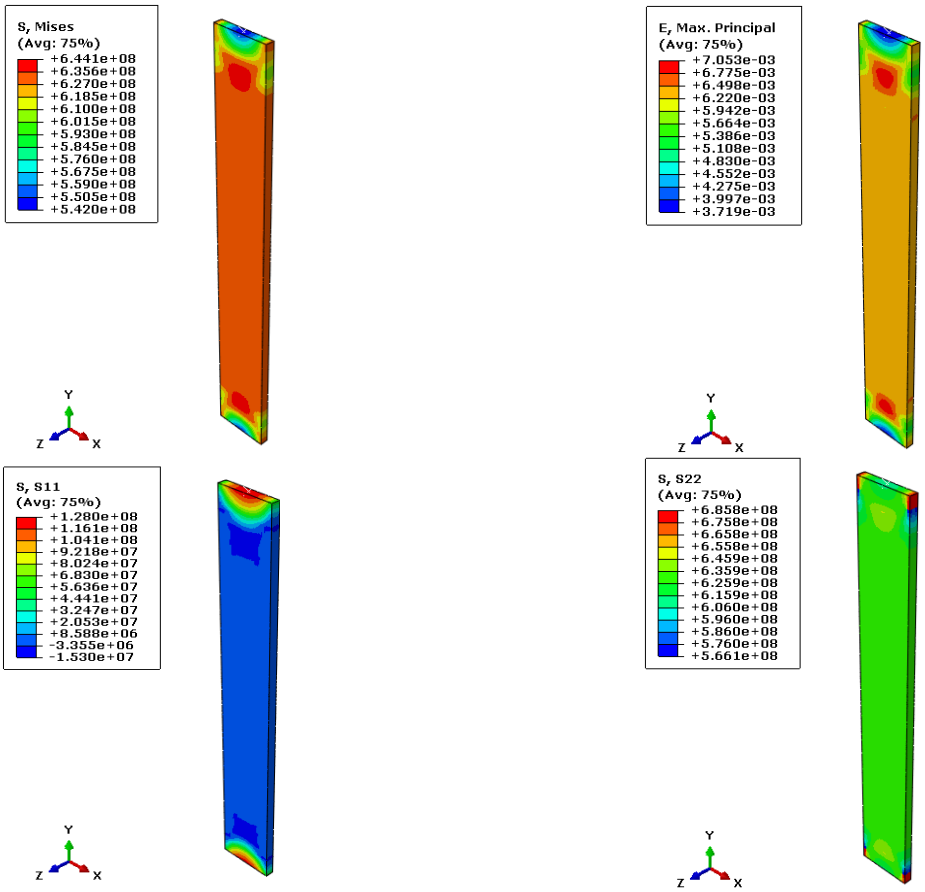

Figure 9. Von Mises stress, maximum principal strain, and S11 and S22 stress contours of Inconel 600

diagram predicted by this research with the laboratory data that the authors conducted in their previous work is depicted in Figure 10.

From Figure 10, there is a reasonable agreement between the fatigue life results obtained using FE method and experiments. A small discrepancy in the result could be attributed to variations in fatigue prediction models, as different models yield slightly different results depending on the material. Additionally, the inherent variability in fatigue phenomena also contributes to minor differences between simulated and experimental results.

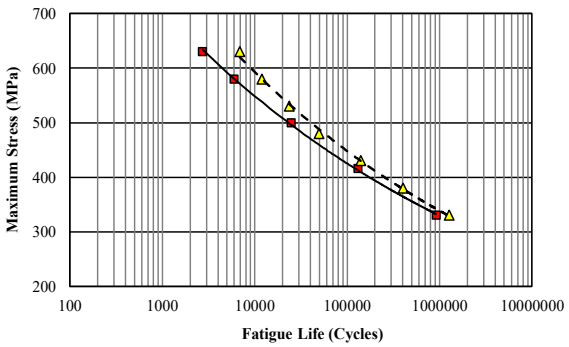

Figure 10. Comparison between the predicted fatigue life of the Inconel 600 standard samples with experimental fatigue test data

4. 2. Multiaxial Fatigue Life Figure 11 presents the hysteresis loops generated in complete loading-unloading combined tension and torsion at each phase angle. The results illustrate significant changes in material response as the phase difference varies. For phase differences between 50° and 60°, the highest material damage was observed, indicating a more critical loading condition. The stress and strain contours at a 50° phase angle between tension and torsion loading are shown in Figure 12. The stress distribution suggests that at this phase angle, the material experiences non-proportional stress components, leading to increased cyclic damage. This is in agreement with previous studies that suggest non-proportional loading accelerates fatigue failure due to the combined effects of normal and shear stress variations.

Next, the FE stress and strain results were imported to MSC.FATIGUE software to predict the fatigue lives based on the previously mentioned critical plane approaches. Figure 13 illustrates the predicted fatigue lives at all phase angles. It was found that:

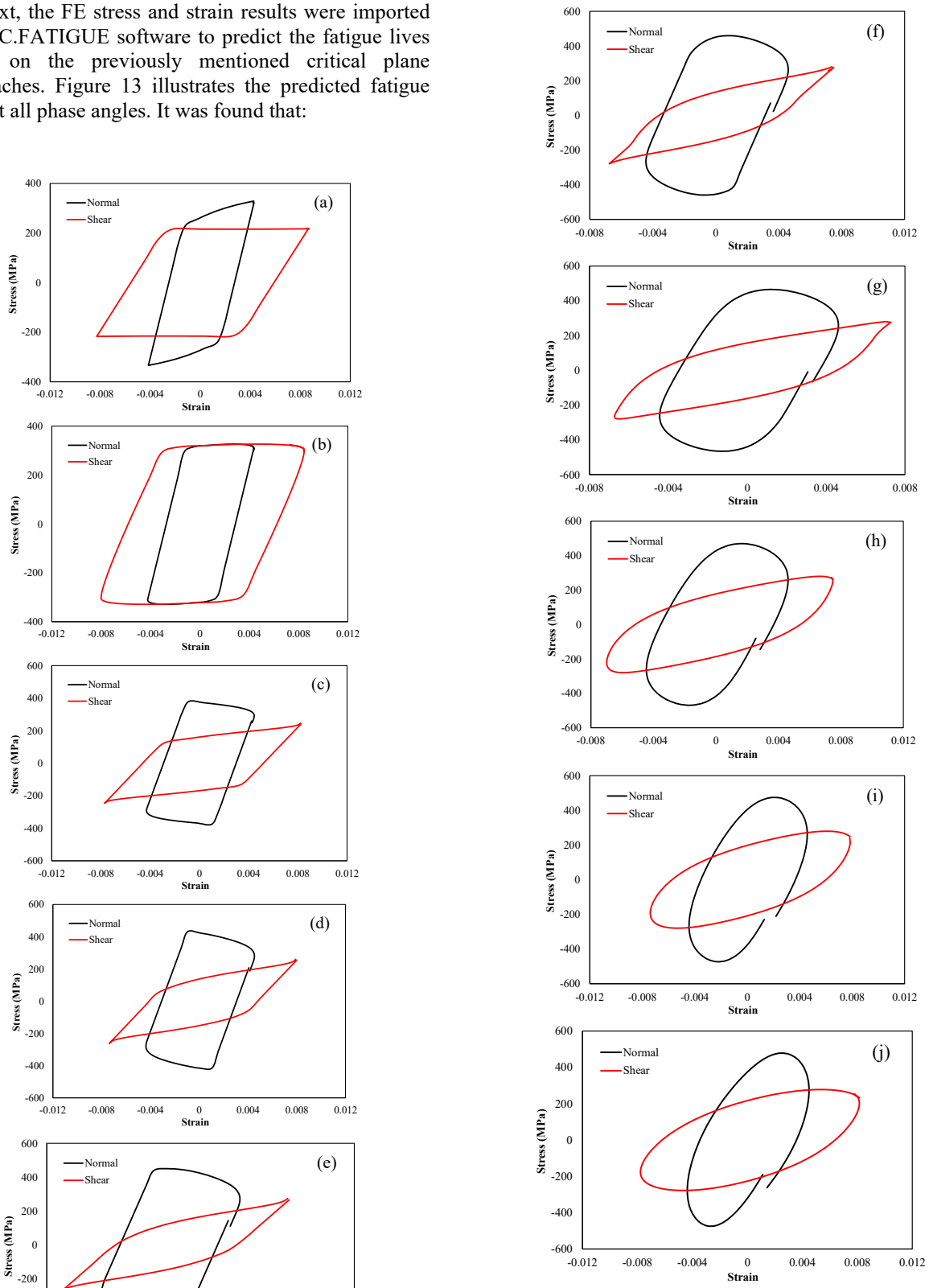

Figure 11. Hysteresis loops generated in complete loading-unloading combined tension and torsion at various phase angle including, (a) in-phase, (b) 10º, (c) 20º, (d) 30º, (e) 40º, (f) 50º, (g) 60º, (h) 70º, (i) 80º, and (j) 90º

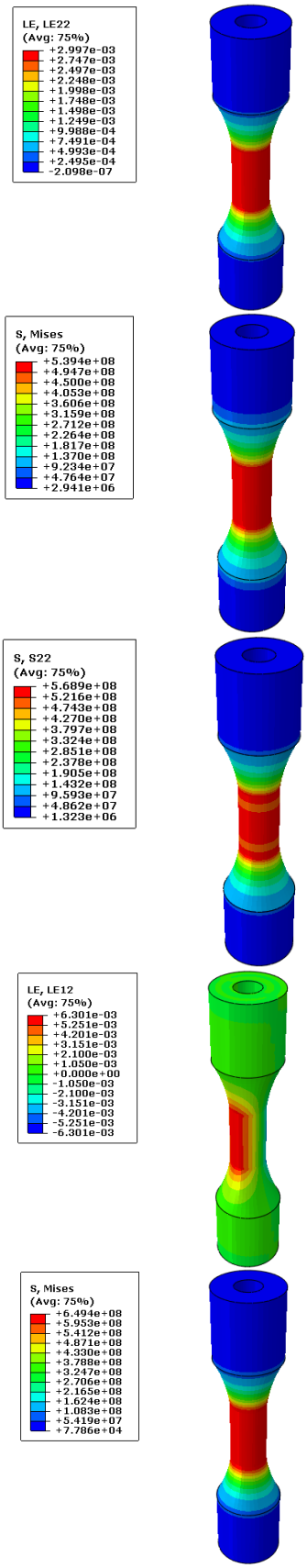

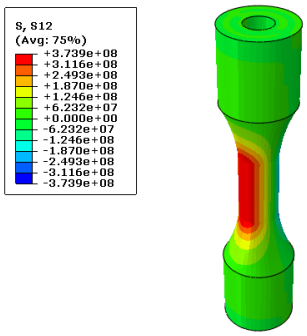

Figure 12. Stress and strain contours at 50º phase angle between tension and torsion loading

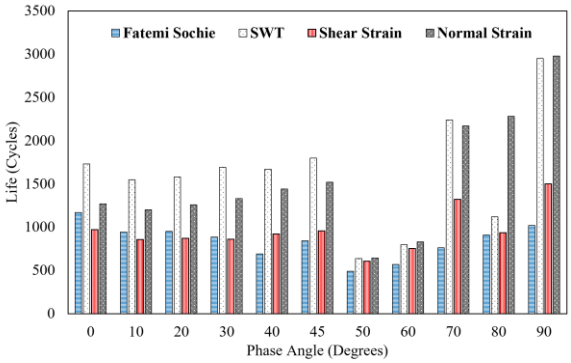

Figure 13. Comparison between the predicted fatigue lives obtained based on different critical plane approaches

- The fatigue life of the Inconel 600 sample was the lowest when subjected to a 50º out-of-phase loading condition.
- The longest fatigue life occurred when two types of loading were perpendicular to each other (i.e., 90° out-of-phase loading condition).

These results suggest that phase difference significantly influences fatigue life, reinforcing the need to consider real loading conditions in engineering applications.

4. 3. Mixed Mode Crack Growth The behavior of a crack under mixed mode loading differs significantly from that under pure mode I (tensile) or mode II (shear) loading. The interaction between the two modes affects crack propagation rate and direction, making predictions more challenging. Figure 14 illustrates the crack paths under different loading conditions, showing that:

- The sample under pure mode II condition exhibited the longest fatigue life before rupture, indicating its higher resistance to crack propagation.
- The sample subjected to pure mode I loading demonstrated the shortest fatigue life, suggesting that tensile loading plays a more dominant role in accelerating crack propagation.

Additionally, Figure 15 displays the crack propagation versus the number of applied cycles until final failure. The crack growth behavior suggests that mode I loading is the most detrimental to the material, while mode II conditions slow down crack propagation. These findings align with existing literature, further validating the numerical model.

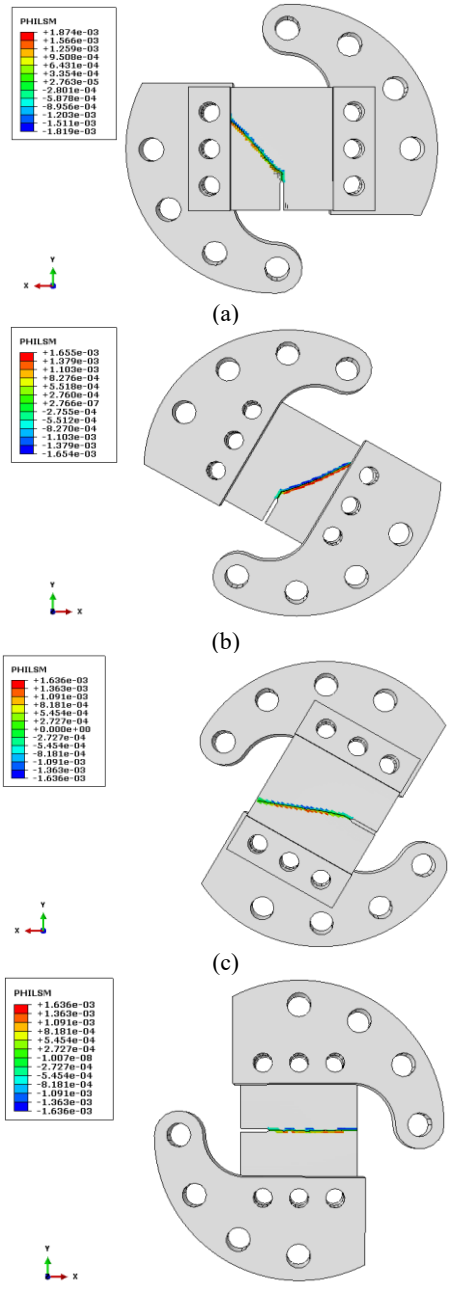

Figure 14. Crack path under different mixed mode conditions, including (a) pure mode II (0 degree) condition, (b) mixed mode I and II (30 degrees) condition, (c) mixed mode I and II (60 degrees) condition, and (d) pure mode I (90 degrees) condition

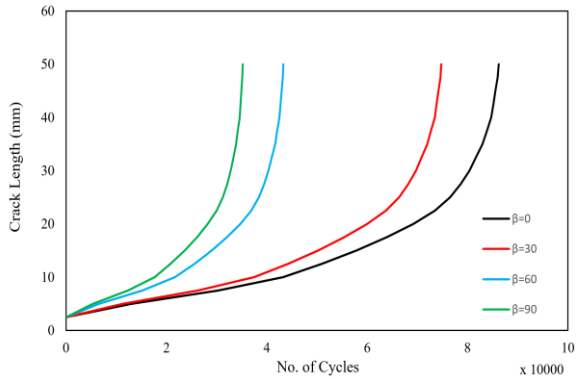

Figure 15. Crack propagation versus the number of applied cycles until final failure

4. 4. Engineering Significance of the Research Results Understanding the multiaxial fatigue life and mixed mode crack growth behavior of Inconel 600 is crucial for high-temperature and high-stress applications. The findings of this research can be applied to:

- Aerospace industry: Components subjected to cyclic thermal and mechanical loading need reliable fatigue life predictions.
- Power plants: Turbine blades and pressure vessels made of Inconel alloys must withstand multiaxial fatigue over extended operational periods.
- Automotive and marine applications: The insights from this study can help optimize the design of components exposed to complex loading conditions.

Beyond these specific industries, the findings have broad implications in various engineering fields. Understanding multiaxial fatigue behavior enables engineers to design safer and more durable components, reducing maintenance costs and preventing catastrophic failures. The results of this study also emphasize the importance of using accurate finite element simulations to predict fatigue behavior, which can reduce the need for expensive and time-consuming experiments. In particular, the results suggest that special consideration should be given to non-proportional loading conditions, as these can lead to accelerated material degradation. Engineers can apply this knowledge to enhance design standards, selecting appropriate fatigue criteria for evaluating life expectancy under different loading scenarios. Additionally, the findings may contribute to the development of new materials with improved fatigue resistance, tailored to high-stress environments.

5. CONCLUSION

This study investigated the multiaxial fatigue and fatigue crack growth behavior of Inconel 600. Fatigue life analysis considered both in-phase and out-of-phase

conditions between tensile and shear stresses. The research employed different critical plane criteria to evaluate fatigue life, while mixed-mode crack growth was analyzed under pure modes I and II and their combinations. The key findings include:

- The results indicated that the fatigue life of the Inconel 600 sample was shortest under a 50º out-of-phase loading condition. Also, the longest fatigue life occurred when the two loading types were perpendicular (90° out-of-phase loading condition).
- The results showed that Fatemi-Socie and shear strain criteria predicted the shortest fatigue lives in phase difference ranges of 0°-30° and 40°-90°, respectively. In addition, it was found that the most critical phase differences were 50° and 60°.
- The sample subjected to pure mode II conditions exhibited the longest fatigue life before rupture, while the sample under pure mode I conditions had the shortest fatigue life.

6. ACKNOWLEDGMENTS

This paper has been supported by the RUDN University Strategic Academic Leadership Program.

7. REFERENCES

1. Nomoto H. Development in materials for ultra-supercritical (USC) and advanced ultra-supercritical (A-USC) steam turbines. Advances in steam turbines for modern power plants: Elsevier; 2017. p. 263-78.
2. Leonard F. Study of stress corrosion cracking of alloy 600 in high temperature high pressure water: The University of Manchester (United Kingdom); 2010.
3. Arghavan A, Reza Kashyzadeh K, Asfarjani AA. Investigating effect of industrial coatings on fatigue damage. Applied Mechanics and Materials. 2011;87:230-7. https://doi.org/10.4028/www.scientific.net/AMM.87.230
4. Kashyzadeh KR, Ghorbani S. Comparison of some selected time-domain fatigue failure criteria dedicated for multi input random non-proportional loading conditions in industrial components. Engineering Failure Analysis. 2023;143:106907. https://doi.org/10.1016/j.engfailanal.2022.106907
5. Fahmi A-TWK, Kashyzadeh KR, Ghorbani S. A comprehensive review on mechanical failures cause vibration in the gas turbine of combined cycle power plants. Engineering Failure Analysis. 2022;134:106094. https://doi.org/10.1016/j.engfailanal.2022.106094
6. Reza Kashyzadeh K, Souri K. A short introduction of blade cooling mechanisms in old gas turbines with the aim of proper distribution of temperature profile. J Adv Therm Sci Res. 2023;10:98-111. https://doi.org/10.15377/2409-5826.2023.10.8
7. Khalid Mohammed Ridha W, Reza Kashyzadeh K, Ghorbani S. Common failures in hydraulic Kaplan turbine blades and practical solutions. Materials. 2023;16(9):3303. https://doi.org/10.3390/ma16093303
8. Kashyzadeh KR, Ghorbani S. High-cycle fatigue behavior and chemical composition empirical relationship of low carbon three-sheet spot-welded joint: An application in automotive industry. Int J Fatigue. 2023;2(1):1-8. https://doi.org/10.62676/p7x1cn02
9. Reza Kashyzadeh K. Effects of axial and multiaxial variable amplitude loading conditions on the fatigue life assessment of automotive steering knuckle. Journal of Failure Analysis and Prevention. 2020;20(2):455-63. https://doi.org/10.1007/s11668-020-00841-w
10. Abdollahnia H, Alizadeh Elizei MH, Reza Kashyzadeh K. Multiaxial fatigue life assessment of integral concrete bridge with a real-scale and complicated geometry due to the simultaneous effects of temperature variations and sea waves clash. Journal of Marine Science and Engineering. 2021;9(12):1433. https://doi.org/10.3390/jmse9121433
11. Xu J, Shang D-G, Sun G-Q, Chen H, Liu E-T. Fatigue life prediction for GH4169 superalloy under multiaxial variable amplitude loading. Journal of Beijing University of Technology. 2012;38(10):1462-6.
12. Kim H, Kim KS, Park H. Ratcheting behavior of Inconel 718 at 649° C under multiaxial loading. Journal of Solid Mechanics and Materials Engineering. 2010;4(1):39-50. https://doi.org/10.1299/jmmp.4.39
13. McDowell DL. Simulation-based strategies for microstructure-sensitive fatigue modeling. Materials Science and Engineering: A. 2007;468:4-14. https://doi.org/10.1016/j.msea.2006.08.129
14. Susmel L, Tovo R, Lazzarin P. The mean stress effect on the high-cycle fatigue strength from a multiaxial fatigue point of view. International Journal of Fatigue. 2005;27(8):928-43. https://doi.org/10.1016/j.ijfatigue.2004.11.012
15. Liu B, Yan X. A new model of multiaxial fatigue life prediction with the influence of different mean stresses. International Journal of Damage Mechanics. 2019;28(9):1323-43. https://doi.org/10.1177/1056789518824396
16. Kashyzadeh KR, Farrahi G, Shariyat M, Ahmadian M. Experimental accuracy assessment of various high-cycle fatigue criteria for a critical component with a complicated geometry and multi-input random non-proportional 3D stress components. Engineering Failure Analysis. 2018;90:534-53. https://doi.org/10.1016/j.engfailanal.2018.03.033
17. Shariyat M. A fatigue model developed by modification of Gough's theory, for random non-proportional loading conditions and three-dimensional stress fields. International journal of fatigue. 2008;30(7):1248-58. https://doi.org/10.1016/j.ijfatigue.2007.08.018
18. Shariyat M. New multiaxial HCF criteria based on instantaneous fatigue damage tracing in components with complicated geometries and random non-proportional loading conditions. International Journal of Damage Mechanics. 2010;19(6):659-90. https://doi.org/10.1177/1056789509338317
19. Yu X, Lin X, Wang Z, Zhang S, Gao X, Zhang Y, et al. Room and high temperature high-cycle fatigue properties of Inconel 718 superalloy prepared using laser directed energy deposition. Materials Science and Engineering: A. 2021;825:141865. https://doi.org/10.1016/j.msea.2021.141865
20. Kawagoishi, Chen, Nisitani. Fatigue strength of Inconel 718 at elevated temperatures. Fatigue & Fracture of Engineering Materials & Structures. 2000;23(3):209-16. https://doi.org/10.1046/j.14602695.2000.00263.x
21. Zhu J-Q, Lu Y-X, Sun L-G, Huang S, Mei L-B, Zhu M-L, et al. Effect of microstructure on fatigue resistance of Inconel 740H and Haynes 282 nickel-based alloys at high temperature. Materials Characterization. 2023;203:113095. https://doi.org/10.1016/j.matchar.2023.113095
22. Maderbacher H, Oberwinkler B, Gänser H-P, Tan W, Rollett M, Stoschka M. The influence of microstructure and operating

temperature on the fatigue endurance of hot forged Inconel® 718 components. Materials Science and Engineering: A. 2013;585:123-31. https://doi.org/10.1016/j.msea.2013.07.053

23. Liu S, Shao S, Guo H, Zong R, Qin C, Fang X. The microstructure and fatigue performance of Inconel 718 produced by laser-based powder bed fusion and post heat treatment. International Journal of Fatigue. 2022;156:106700. https://doi.org/10.1016/j.ijfatigue.2021.106700
24. Antunes F, Ferreira J, Branco C. High temperature fatigue crack growth in Inconel 718. Materials at High Temperatures. 2000;17(4):439-48. https://doi.org/10.1179/mht.2000.058
25. Antunes F, Ferreira J, Branco C, Byrne J. Influence of stress state on high temperature fatigue crack growth in Inconel 718. Fatigue & Fracture of Engineering Materials & Structures. 2001;24(2):127-35. https://doi.org/10.1046/j.1460-2695.2001.00375.x
26. Gustafsson D, Lundström E. High temperature fatigue crack growth behaviour of Inconel 718 under hold time and overload conditions. International Journal of Fatigue. 2013;48:178-86. https://doi.org/10.1016/j.ijfatigue.2012.10.018
27. Ghonem H, Nicholas T, Pineau A. Elevated temperature fatigue crack growth in alloy 718—part II: effects of environmental and material variables. Fatigue & Fracture of Engineering Materials & Structures. 1993;16(6):577-90. https://doi.org/10.1016/0025-5416(81)90225-8
28. Meggiolaro M, Castro J. Statistical evaluation of strain-life fatigue crack initiation predictions. International Journal of Fatigue. 2004;26(5):463-76. https://doi.org/10.1016/j.ijfatigue.2003.11.004
29. Rasul A, Karuppanan S, Perumal V, Ovinis M, Iqbal M. Multi-objective optimization of stress concentration factors for fatigue design of internal ring-reinforced KT-joints undergoing brace axial compression. Civ Eng J. 2024;10:1742-64. https://doi.org/10.28991/CEJ-2024-010-06-03
30. Major Z, Bodnár L, Merczel DB, Szép J, Lublóy É. Analysis of the heating of steel structures during fire load. 2024. https://doi.org/10.28991/ESJ-2024-08-01-01
31. Rahmani M, Petrudi AM. Investigation of Crack Growth by Loading Fatigue due to Fluid and Structural Coupling Vibrations in the Joint of Thermowell Welding in Gas Pipeline. http://dx.doi.org/10.46565/jreas.2020.v05i02.001
32. Carpinteri A, Spagnoli A, Vantadori S. Multiaxial fatigue assessment using a simplified critical plane-based criterion. International Journal of Fatigue. 2011;33(8):969-76. https://doi.org/10.1016/j.ijfatigue.2011.01.004
33. Carpinteri A, Spagnoli A, Vantadori S. Multiaxial fatigue life estimation in welded joints using the critical plane approach. International Journal of Fatigue. 2009;31(1):188-96. https://doi.org/10.1016/j.ijfatigue.2008.03.024
34. Kashyzadeh KR. Utilizing data-driven methods to predict the fatigue life of cement concrete considering corrosive environmental factors. Journal of Design Against Fatigue. 2023;1(3). https://doi.org/10.62676/3th69185
35. Fatemi A, Socie DF. A critical plane approach to multiaxial fatigue damage including out-of-phase loading. Fatigue & Fracture of Engineering materials & structures. 1988;11(3):149-65. https://doi.org/10.1111/j.1460-2695.1988.tb01169.x
36. Myler P, Wyatt LM. Mechanics of solids. Mechanical Engineer's Reference Book: Elsevier; 1994. p. 8-1-8-42.
37. Dowling NE, Kampe SL, Kral MV. Mechanical behavior of materials: engineering methods for deformation, fracture, and fatigue. (no Title). 2007.
38. Riemer A, Leuders S, Thöne M, Richard H, Tröster T, Niendorf T. On the fatigue crack growth behavior in 316L stainless steel manufactured by selective laser melting. Engineering Fracture Mechanics. 2014;120:15-25. https://doi.org/10.1016/j.engfracmech.2014.03.008
39. Dahar MS, Seifi SM, Bewlay B, Lewandowski JJ. Effects of test orientation on fracture and fatigue crack growth behavior of third generation as-cast Ti–48Al–2Nb–2Cr. Intermetallics. 2015;57:73-82. https://doi.org/10.1016/j.intermet.2014.10.005
40. Ritchie R, Knott J. Mechanisms of fatigue crack growth in low alloy steel. Acta Metallurgica. 1973;21(5):639-48. https://doi.org/10.1016/0001-6160(73)90073-4
41. Zinsser W, Lewandowski J. Effects of R-ratio on the fatigue crack growth of Nb-Si (ss) and Nb-10Si In Situ composites. Metallurgical and Materials transactions A. 1998;29:1749-57. https://doi.org/10.1007/s11661-998-0098-x
42. Maiti S, Geubelle PH. A cohesive model for fatigue failure of polymers. Engineering Fracture Mechanics. 2005;72(5):691-708. https://doi.org/10.1016/j.engfracmech.2004.06.005
43. Kirane K, Bažant ZP. Size effect in Paris law and fatigue lifetimes for quasibrittle materials: Modified theory, experiments and micro-modeling. International Journal of Fatigue. 2016;83:209-20. https://doi.org/10.1016/j.ijfatigue.2015.10.015
44. Kujawski D. Correlating R-ratio effects on FCG behavior using ΔKd function. Theoretical and Applied Fracture Mechanics. 2022;118:103244. https://doi.org/10.1016/j.tafmec.2021.103244
45. Ding J, Hall R, Byrne J. Effects of stress ratio and temperature on fatigue crack growth in a Ti–6Al–4V alloy. International journal of fatigue. 2005;27(10-12):1551-8. https://doi.org/10.1016/j.ijfatigue.2005.06.007
46. ASTM A. E2207–08, Standard practice for strain-controlled axialtorsional fatigue testing with thin-walled tubular specimens. ASTM International, West Conshohocken (PA, USA): Book of Standards. 2008;3. https://www.astm.org/e2207-15r21.html
47. Khalil Z, Elghazouli AY, Martinez-Paneda E. A generalised phase field model for fatigue crack growth in elastic–plastic solids with an efficient monolithic solver. Computer Methods in Applied Mechanics and Engineering. 2022;388:114286. https://doi.org/10.1016/j.cma.2021.114286
48. Oskui AEh, Choupani N, Shameli M. 3D characterization of mixed-mode fracture toughness of materials using a new loading device. Latin American Journal of Solids and Structures. 2016;13:1464-82. https://doi.org/10.1590/1679-78252779
49. Choupani N. Experimental and numerical investigation of the mixed-mode delamination in Arcan laminated specimens. Materials Science and Engineering: A. 2008;478(1-2):229-42. https://doi.org/10.1016/j.msea.2007.05.103
50. Karthik D, Swaroop S. Laser shock peening enhanced corrosion properties in a nickel based Inconel 600 superalloy. Journal of Alloys and Compounds. 2017;694:1309-19.
51. Moradi A, Ghorbani S, Chizari M. Experimental research on mechanical, material, and metallurgical properties of Inconel 600: Application in elevated temperature environment. Journal of Design Against Fatigue. 2024;2(1). https://doi.org/10.62676/jdaf.2024.2.1.30
52. Kashyzadeh KR, Farrahi G, Shariyat M, Ahmadian M. Experimental and finite element studies on free vibration of automotive steering knuckle. International Journal of Engineering Transactions B: Applications. 2017;30:1776-83. https://doi.org/10.5829/ije.2017.30.11b.20

Persian Abstract

چکیده

این مطالعه به بررسی پیش‌بینی عمر خستگی اینکونل ۶۰۰ در شرایط بارگذاری چند محوری و همچنین رشد ترک خستگی در حالت مود ترکیبی I و II می‌پردازد. شبیه‌سازی اجزای محدود بر اساس معیارهای صفحه بحرانی برای تحلیل خستگی تحت بارگذاری ترکیبی کشش و برش در حالت‌های مختلف غیرمتناسب (یعنی اختلاف فاز بین بارهای کششی و برشی) انجام شد. برای دستیابی به این امر، تنش کششی کاملا معکوس شونده با حداکثر مقدار ۴۸۰ مگاپاسکال (میانگین تنش: صفر) در نظر گرفته شد. پس از آن، تنش برشی ثابت ۲۸ مگاپاسکال در زوایای فاز مختلف از ۰ تا ۹۰ درجه در فواصل ۱۰ درجه (یعنی $0°\leq\theta\leq90°$, $\Delta\theta=10°$) اعمال شد. برای همه حالت‌ها، نمودارهای تنش هیسترزیس برای بررسی رفتار چرخه‌ای ماده استخراج شد. علاوه بر این، مدل‌های آسیب خستگی مختلف، مانند فاطمی–سوشی، اسمیت–واتسون–تاپر، کرنش معمولی و کرنش برشی، برای ارزیابی عمر خستگی نمونه‌ها در حالت‌های بارگذاری مختلف از طریق نرم‌افزار ام–اف–سی استفاده شد. نتایج نشان داد که معیارهای فاطمی–سوشی و کرنش برشی کوتاه ترین عمر خستگی را برای اختلاف فاز به ترتیب در محدوده ۰–۳۰ درجه و ۴۰–۹۰ درجه گزارش می‌کنند. بنابراین، انتخاب یک معیار محافظه کارانه‌تر مطلقاً غیرممکن است و بستگی به شرایط بارگذاری دارد. علاوه بر این مشخص شد که بحرانی ترین وضعیت مربوط به اختلاف فاز ۵۰ درجه و ۶۰ درجه است. سپس به منظور بررسی عددی رفتار رشد ترک، از مدل فیکسچر نیمه آرکان استفاده شد. شبیه‌سازی‌ها برای چهار حالت بارگذاری مختلف (یعنی تنظیمات فیکسچر)، با در نظر گرفتن تغییرات در زاویه بارگذاری با محور طولی ترک (۰، ۳۰، ۶۰ و ۹۰ درجه) انجام شد. در نهایت نمودارهای طول ترک بر حسب چرخه بارگذاری استخراج شدند. نتایج نشان داد که کمترین و بیشترین نرخ رشد ترک زمانی رخ می‌دهد که زاویه بین بارگذاری و محور طولی ترک به ترتیب ۰ و ۹۰ درجه باشد.